

## Corrosion Inhibition Effect of Methanol Extract of Nerium Oleander on Copper in Nitric Acid Solutions

A.S. Fouda<sup>1,\*</sup>, H.M. Elabbasy<sup>2</sup>

<sup>1</sup> Department chemistry, Faculty of Science, Mansoura University, Mansoura-35516, Egypt.

<sup>2</sup> Misr higher Institute for Engineering and Technology, Mansoura, Egypt.

\*E-mail: [asfouda@hotmail.com](mailto:asfouda@hotmail.com), [helabbasy@hotmail.com](mailto:helabbasy@hotmail.com)

Received: 18 February 2019 / Accepted: 18 April 2019 / Published: 10 June 2019

---

Corrosion inhibition and adsorption studies of methanol extract of Nerium oleander for Cu in 0.5 M HNO<sub>3</sub> have been studied by weight loss and electrochemical techniques. Effect of temperature from 30 to 50°C on inhibition action of Nerium oleander extract (NOE) was studied. The inhibition efficiency (IE) of NOE increases with increasing its concentration. The adsorption process and IE were preferred at lower temperatures. Larger negative value of standard free energy was obtained at lower temperature. The polarization data indicated that NOE acts as a mixed type inhibitor. Adsorption isotherm obeyed Frumkin isotherm and NOE was adsorbed physically on the Cu surface. The surface morphology was investigated by scanning electron microscopy (SEM).

---

**Keywords:** Nerium oleander, Cu, Adsorption, EIS, SEM.

### 1. INTRODUCTION

The study of Cu corrosion inhibition is of high importance due to it used widely in various industrial operations. Cu and its alloys used in production of integrated circuits as they have premium thermal and electrical conductivity [1,2]. Cu is considered a noble metal and its corrosion needs strong oxidants. The most effective medium is nitric acid solution, so the use of this medium on copper was included in a great deal of research [3-8]. The development and investigation of organic compounds as corrosion inhibitors is of great importance, as these compounds have heteroatoms (N, O, S,), also contain multiple bonds through which the adsorption on the metal surface takes place. The molecular structure of organic compounds is high which leads to a great influence on the extent of corrosion inhibition [9-12]. Recently, green substances are greatly used as corrosion inhibitors for some metals because they are nontoxic, biodegradable, renewable, cheap, and easy handling. Numerous authors were interested in the usage of the plant extracts for corrosion inhibition of metals and alloys, especially for Cu corrosion

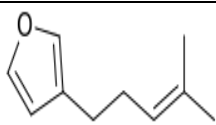
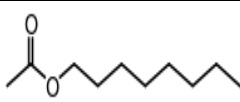

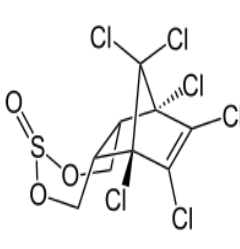
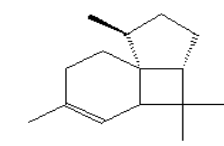
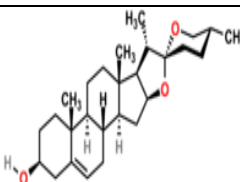
in various acidic solutions [13-21]. Nerium oleander (NOE) is a plant extract applied in the current study as an inhibitor for Cu corrosion in 0.5 M HNO<sub>3</sub> solution.

## 2. EXPERIMENTAL TECHNIQUES

### 2.1 Preparation of the extract

A mixture of 500 g of NOE powder with 900 ml methanol was kept for two weeks at room temperature, then allowed to dry in shade through air-tight glass container. After filtration, the filtrate was put in front of a fan at room temperature to complete dryness, then kept in an air-tight container for using. Gas chromatography and mass spectroscopy analysis of methanolic extract of NOE indicate the main chemical constituents that characterized in Table 1.

**Table 1.** Some of the main photo components identified in the methanol extract of NOE

Name	Structural formula	IUPAC Name	Molecular formula	Molar Mass, g/mol
Perillene		3-(4-Methyl-3-pentenyl)furan	C <sub>10</sub> H <sub>14</sub> O	150.22
Octyl acetate		Octyl acetate	C <sub>10</sub> H <sub>20</sub> O <sub>2</sub>	172.26
2-Nonanol		nonan-2-ol	C <sub>9</sub> H <sub>20</sub> O	144.25
Endosulfan II		6,7,8,9,10,10-Hexachloro-1,5,5a,6,9,9a-hexahydro-6,9-methano-2,4,3-benzodioxathiepine-3-oxide	C <sub>9</sub> H <sub>6</sub> Cl <sub>6</sub> O <sub>3</sub> S	406.93
Tetratetracontane	CH <sub>3</sub> (CH <sub>2</sub> ) <sub>42</sub> CH <sub>3</sub>	Tetratetracontane	C <sub>44</sub> H <sub>90</sub>	619.19
Italicene		Italicene	C <sub>15</sub> H <sub>24</sub>	204.35
Diosgenin		(3β,25R)-spirost-5-en-3-ol	C <sub>27</sub> H <sub>42</sub> O <sub>3</sub>	414.62

## 2.2 Cu specimens and solutions

Cu specimens (whose composition as weight percentage is given as: 0.0005% Bi, 0.001% Sn, 0.002% Pb, 0.001% Ag, 0.01% Fe, 0.0002% other elements and Cu is the rest) of dimensions  $3 \times 1 \times 2$  cm<sup>2</sup> were abraded using different grades of emery papers then degreased using methanol [22]. The concentration of the applied corrosive solutions, that prepared from AR grade HNO<sub>3</sub> (7 M), was checked using standardized NaOH. In order to obtain 0.5 M HNO<sub>3</sub>, bidistilled water was used for dilution. 1000 ppm stock solution of NOE was obtained by dissolving 1 gm of NOE in 1000 ml of absolute methanol. The wanted concentrations (5–25 ppm) were then attained using bidistilled water for dilution.

## 2.3 Weight loss (WL) method

The Cu metal coupons were weighed then immersing in 100 test solutions without and with NOE for 3 hrs. The weight of the specimens was taken again after immersion. The %IE of Nerium oleander extract and the copper surface coverage ( $\theta$ ) were calculated as follows:

$$\%IE = \theta \times 100 = \left[1 - \frac{W_{inh}}{W_{free}}\right] \times 100 \quad (1)$$

where  $W_{free}$  and  $W_{inh}$  are the WL's of Cu without and with NOE, respectively.

## 2.4 Electrochemical techniques

A cell of three electrodes was employed in electrochemical measurements. Pt foil was used as the auxiliary electrode and a saturated calomel electrode (SCE) was used as the reference electrode. The Cu working electrode cutting from Cu sheet was prepared to have a surface area equals 1 cm<sup>2</sup>. The Cu electrode surface was abraded and cleaned as explained in the WL method. The electrochemical techniques have been performed using PCI4-G750 Potentiostat/Galvanostat with a personal computer has Gamry PCI4-G750 software for calculations. All electrochemical studies were performed at 30°C  $\pm 1$  and the results were always repeated minimum three times for precision. Before tests, a time period of about 30 minutes was given at first until a steady state was reached.

### 2.4.1 Potentiodynamic polarization (PP) tests

Potentiodynamic measurements were performed at a scan rate of 1 mVs<sup>-1</sup> from a more negative potential to more positive potential than open circuit potential ( $E_{ocp}$ ). Corrosion potential ( $E_{corr}$ ) and corrosion current densities ( $i_{corr}$ ) were determined at Tafel regions. Values of  $i_{corr}$  were used for calculating values of %IE and  $\theta$  as below:

$$\%IE = \theta \times 100 = \left[1 - \frac{i_{corr(inh)}}{i_{corr(free)}}\right] \times 100 \quad (2)$$

Where  $i_{corr(free)}$  and  $i_{corr(inh)}$  are corrosion current densities without and with NOE, respectively.

#### 2.4.2 Electrochemical impedance spectroscopy (EIS) tests

EIS tests were performed in the range between  $10^5$  and  $10^{-1}$  Hz at  $E_{ocp}$  through AC signal of small amplitude 10 mV peak to peak. The charge transfer resistance ( $R_{ct}$ ) and the double layer capacitance ( $C_{dl}$ ) were obtained from the EIS plots.  $R_{ct}$  was employed in calculating %IE and  $\theta$  as follows:

$$\%IE = \theta \times 100 = \left[1 - \frac{R_{ct(\text{free})}}{R_{ct(\text{inh})}}\right] \times 100 \quad (3)$$

where  $R_{ct(\text{free})}$  and  $R_{ct(\text{inh})}$  are charge transfer resistance without and with NOE, respectively.

#### 2.4.3 Electrochemical frequency modulation (EFM) tests

EFM tests took place by applying 10 mV perturbation signal with two sine waves of 2 and 5 Hz. Values of  $i_{corr}$ , Tafel slopes ( $\beta_c$  and  $\beta_a$ ) and the causality factors (CF-2 and CF-3) were determined from the bigger peaks. Values of  $\theta$  and %IE were calculated by applying equation (2).

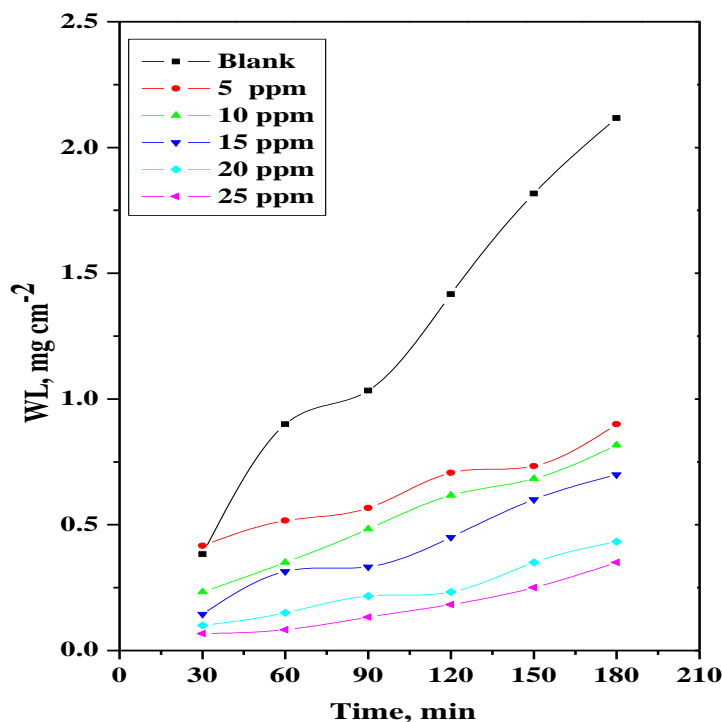
#### 2.5 Surface Morphology Studies

The surface morphology studies were performed using JEOL JSM-5500 scanning electron microscope. The Cu specimens were treated as described in WL method, then exposed to 0.5 M  $\text{HNO}_3$  test solutions without and with NOE for 24 hours. Energy dispersive X-ray (EDX) was used to indicate the elements present on the Cu surface after 24 hours of exposure to the uninhibited and inhibited 0.5  $\text{HNO}_3$  solutions.

### 3. RESULT AND DISCUSSION

#### 3.1 Weight loss (WL) method

Fig. 1 displays the change of WL of the Cu with time in 0.5  $\text{HNO}_3$  without and with different concentrations of NOE at 30°C. It is clear from the figure that the WL of the Cu decreases with increasing NOE concentration, this means that NOE is an effective inhibitor of Cu corrosion in  $\text{HNO}_3$ .



**Figure 1.** Change of WL of the Cu with time in 0.5 HNO<sub>3</sub> without and with different concentrations of NOE at 30°C

### 3.2 Influence of Temperature

WL method was used to check the influence of temperature on the corrosion rate (CR), metal WL,  $\theta$ , and %IE for Cu in 0.5 M HNO<sub>3</sub> without and with different concentrations of NOE at a temperature range (30-50°C) (Table 2). The increase in CR and WL with increasing temperature is indicating physical adsorption [23] of NOE on the Cu surface. Table 2 indicates that %IE increases with adding more NOE, while decreases with raising the temperature. This might because the increase in temperature may stimulate larger kinetic energy of metal surface, that reduce the adsorption process while support the desorption process, hence the equilibrium move towards desorption [24].

**Table 2.** Influence of temperature on CR, WL,  $\theta$ , and %IE for Cu in 0.5 HNO<sub>3</sub> without and with different concentrations of NOE

Temp., °C	C <sub>inh</sub> , Ppm	WL, mg cm <sup>-2</sup>	CR, mg cm <sup>-2</sup> min <sup>-1</sup>	$\theta$	%IE
30	Blank	1.417	0.012	—	—
	5	0.707	0.006	0.501	50.1
	10	0.617	0.005	0.565	56.5
	15	0.450	0.004	0.682	68.2
	20	0.233	0.002	0.836	83.6
	25	0.183	0.002	0.871	87.1
35	Blank	2.086	0.017	—	—
	5	1.050	0.009	0.497	49.7
	10	0.950	0.008	0.545	54.5

	15	0.683	0.006	0.673	67.3
	20	0.380	0.003	0.818	81.8
	25	0.300	0.003	0.856	85.6
40	Blank	1.650	0.014	—	—
	5	1.267	0.011	0.232	23.2
	10	0.967	0.008	0.414	41.4
	15	0.552	0.005	0.666	66.6
	20	0.433	0.004	0.738	73.8
	25	0.367	0.003	0.778	77.8
45	Blank	4.828	0.040	—	—
	5	3.790	0.032	0.215	21.5
	10	2.950	0.025	0.389	38.9
	15	1.700	0.014	0.648	64.8
	20	1.700	0.014	0.648	64.8
	25	1.317	0.011	0.727	72.7
50	Blank	5.600	0.047	—	—
	5	4.983	0.042	0.110	11.0
	10	3.667	0.031	0.345	34.5
	15	2.267	0.019	0.595	59.5
	20	1.967	0.016	0.649	64.9
	25	1.847	0.015	0.670	67.0

The thermodynamic activation parameters of the corrosion process of Cu in 0.5 M HNO<sub>3</sub> were determined by plots of log CR against 1/T (Fig. 2) and log (CR /T) against 1/T (Fig. 3) according to Arrhenius-type equation (Eq.4) and transition-state equation (Eq.5) [25,26]:

$$CR = Ae^{\frac{-E_a^*}{RT}} \quad (4)$$

$$CR = \frac{RT}{Nh} e^{\frac{\Delta S^*}{R}} e^{\frac{-\Delta H^*}{RT}} \quad (5)$$

Where A is frequency factor, E<sub>a</sub><sup>\*</sup> is activation energy, R is gas constant, T is absolute temperature, N is Avogadro's number, h is Planck's constant, ΔS<sup>\*</sup> is entropy of activation and ΔH<sup>\*</sup> is enthalpy of activation. The calculated values of thermodynamic activation parameters (E<sub>a</sub><sup>\*</sup>, ΔS<sup>\*</sup>, ΔH<sup>\*</sup>) were listed in Table 3. The results indicate that E<sub>a</sub><sup>\*</sup> in inhibited solutions are higher than it in uninhibited one, that suggests physisorption of NOE on Cu surface [27]. Higher values of E<sub>a</sub><sup>\*</sup> in inhibited solutions could also be associated with the increase in thickness of the double layer, that increases the E<sub>a</sub><sup>\*</sup> of the corrosion process [28]. The positive sign of ΔH<sup>\*</sup> indicates endothermic corrosion process. Negative ΔS<sup>\*</sup> values indicate a decrease in disordering at moving from reactants to the activated complex [29]. Shifting of ΔS<sup>\*</sup> to more positive values with increasing NOE concentration may referred to the driving force that can overcome the barriers for the adsorption of NOE on the Cu surface.

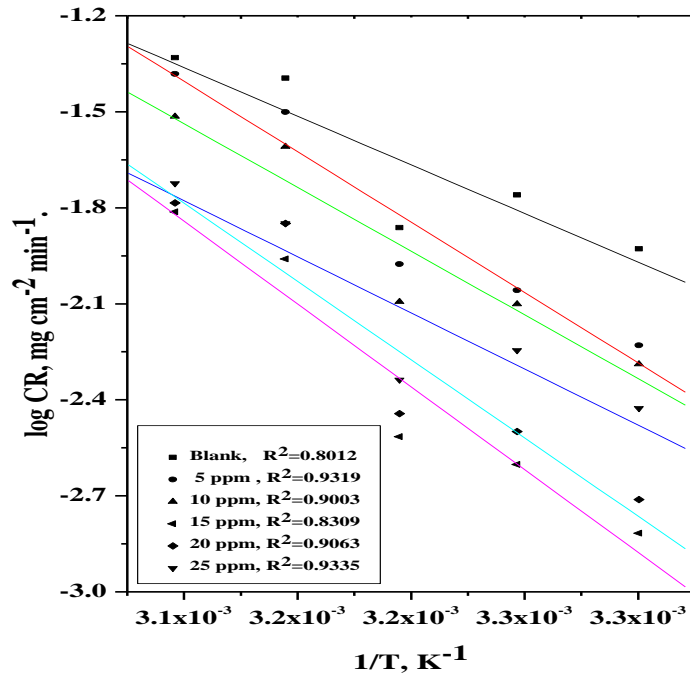


Figure 2. log CR against 1/T for Cu in 0.5 M HNO<sub>3</sub> without and with different concentrations of NOE

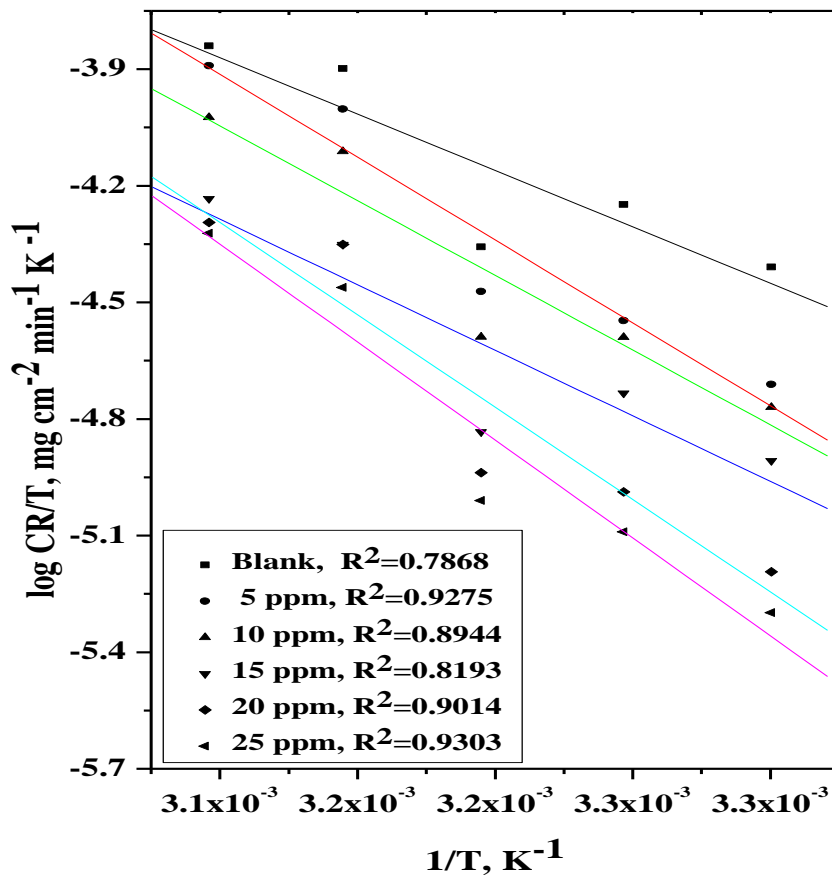


Figure 3. Log (CR/T) against 1/T for Cu in 0.5 M HNO<sub>3</sub> without and with different concentrations of NOE

**Table 3.** Thermodynamic activation parameters as resulted from Arrhenius-type and transition-state equations

$C_{inh}$ , ppm	$A$ , $mg\ cm^{-2}\ min^{-1}$	$E_a^*$ , $kJ\ mol^{-1}$	$\Delta H^*$ , $kJ\ mol^{-1}$	$\Delta S^*$ , $J\ mol^{-1}\ K^{-1}$
Blank	8.061	58.2	26.6	-81.5
5	12.235	84.2	35.5	-19.3
10	10.810	76.3	32.0	-46.7
15	9.097	67.2	28.0	-79.4
20	13.382	93.7	39.5	+2.5
25	14.202	99.1	41.9	+18.3

### 3.3 Adsorption Isotherms

Several adsorption isotherms were applied to fit the data obtained from WL method. Frumkin model was the best one. According to Frumkin isotherm, the relationship between  $\theta$  and NOE concentration is as follows:

$$\ln\left(\frac{C_{inh}\theta}{1-\theta}\right) = \ln K_{ads} + 2a\theta \quad (6)$$

where  $K_{ads}$  is adsorption constant and  $a$  is the interaction parameter between adsorbed species on the surface. Straight lines, with slopes equal ( $2a$ ) and intercepts equal ( $\ln K_{ads}$ ), were obtained by plotting  $\ln [C_{inh}\theta / (1 - \theta)]$  vs.  $\theta$  as illustrated in Fig. 4.  $\ln K_{ads}$  is related to the standard free energy of adsorption ( $\Delta G^{\circ}_{ads}$ ) by the following equation:

$$\ln K_{ads} = \ln 0.018 - \frac{\Delta G^{\circ}_{ads}}{R} \frac{1}{T} \quad (7)$$

where 0.018 is the molar concentration of water in solution. Standard enthalpy of adsorption ( $\Delta H^{\circ}_{ads}$ ) was attained by applying the following relation [30]:

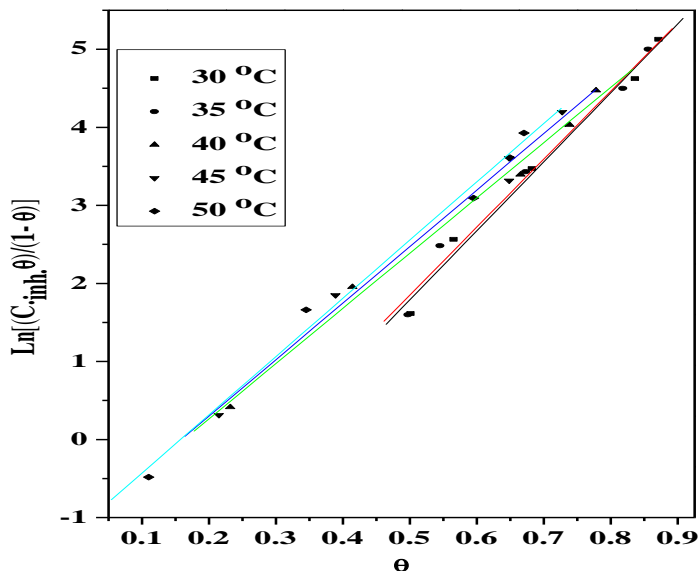
$$\ln K_{ads} = -\frac{\Delta H^{\circ}_{ads}}{RT} + \text{constant} \quad (8)$$

Plotting  $\ln K_{ads}$  vs.  $1/T$  result in a straight line with slope equals ( $-\Delta H^{\circ}_{ads} / R$ ) as illustrated in Fig. 5. Standard entropy of adsorption ( $\Delta S^{\circ}_{ads}$ ) can be determined as follows [31]:

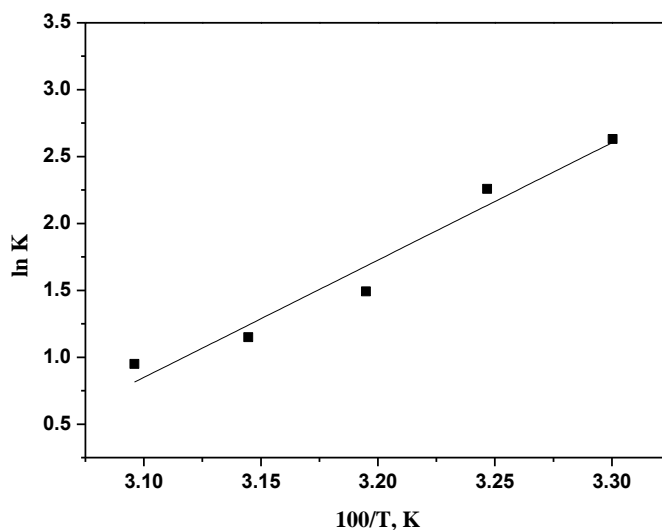
$$\Delta S^{\circ}_{ads} = \frac{\Delta H^{\circ}_{ads} - \Delta G^{\circ}_{ads}}{T} \quad (9)$$

The adsorption results were given in Table 4. Values of ( $a$ ) are positive, indicating attractive forces formed between the adsorbed NOE molecules on the Cu surface. Values of  $\Delta G^{\circ}_{ads}$  were low (less than  $20\ kJ\ mol^{-1}$ ) indicating physical adsorption of NOE on the Cu surface. Negative  $\Delta H^{\circ}_{ads}$  values are indicating exothermic adsorption process [32]. The values of  $\Delta S^{\circ}_{ads}$  are negative as accompanied with exothermic adsorption process.





**Figure 4.** Plots of Frumkin adsorption isotherm at different temperatures for Cu in 0.5 M HNO<sub>3</sub> without and with different concentrations of NOE



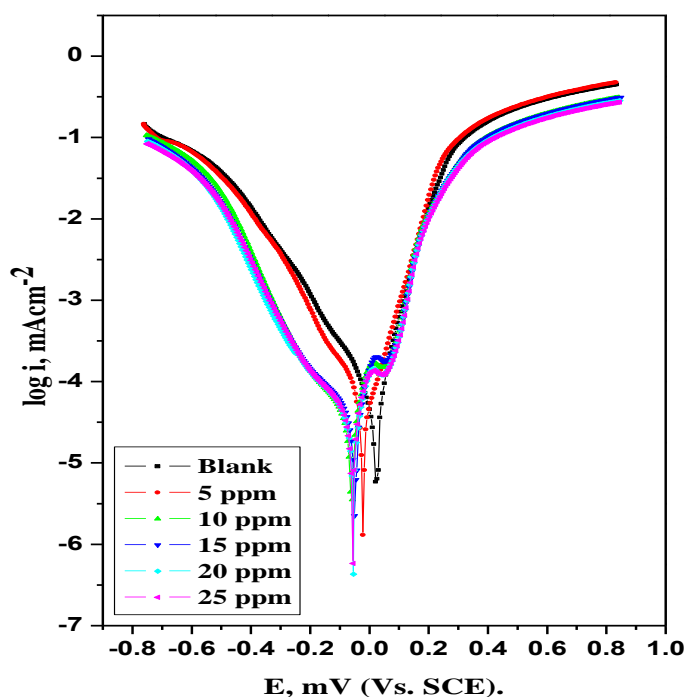
**Figure 5.**  $\ln K_{ads}$  against  $1000/T$  for Cu in 0.5 M HNO<sub>3</sub>

**Table 4.** Results from Frumkin adsorption model at different temperatures for Cu in 0.5 M HNO<sub>3</sub> without and with different concentrations of NOE

Temp., °C	A	$K_{ads}, M^{-1}$	$-\Delta G^{\circ}_{ads}, kJ mol^{-1}$	$-\Delta H^{\circ}_{ads}, kJ mol^{-1}$	$-\Delta S^{\circ}_{ads}, J mol^{-1}K^{-1}$
30	8.840	13.874	16.7	72.9	185.3
35	8.716	9.564	16.1		184.5
40	7.083	4.442	14.3		187.1
45	7.246	3.155	13.7		186.3
50	7.469	2.586	13.3		184.4

### 3.4 Potentiodynamic polarization (PP) measurements

Anodic and cathodic PP curves for Cu corrosion in 0.5 M HNO<sub>3</sub> without and with different concentrations of NOE at 30°C were shown in Fig. 6. Kinetic parameters derived from the polarization curves (such as  $E_{\text{corr}}$ ,  $i_{\text{corr}}$ ,  $\beta_a$  and  $\beta_c$ , CR,  $\theta$  and % IE) were given in Table 5. It is concluded from the experimental potentiodynamic results that the presence of NOE affects both the anodic and the cathodic reactions, which means that NOE behaved as a mixed-type inhibitor. Unchanging of  $\beta_a$  and  $\beta_c$  upon addition of NOE indicates that this extract blocks the metal surface reaction sites without affecting the reactions mechanisms. The data in Table 5 indicated increasing of % IE and decreasing of CR with increasing of concentration of NOE.



**Figure 6.** Anodic and cathodic PP curves for Cu in 0.5 M HNO<sub>3</sub> without and with different concentrations of NOE

**Table 5.** Kinetic parameters derived from PP curves

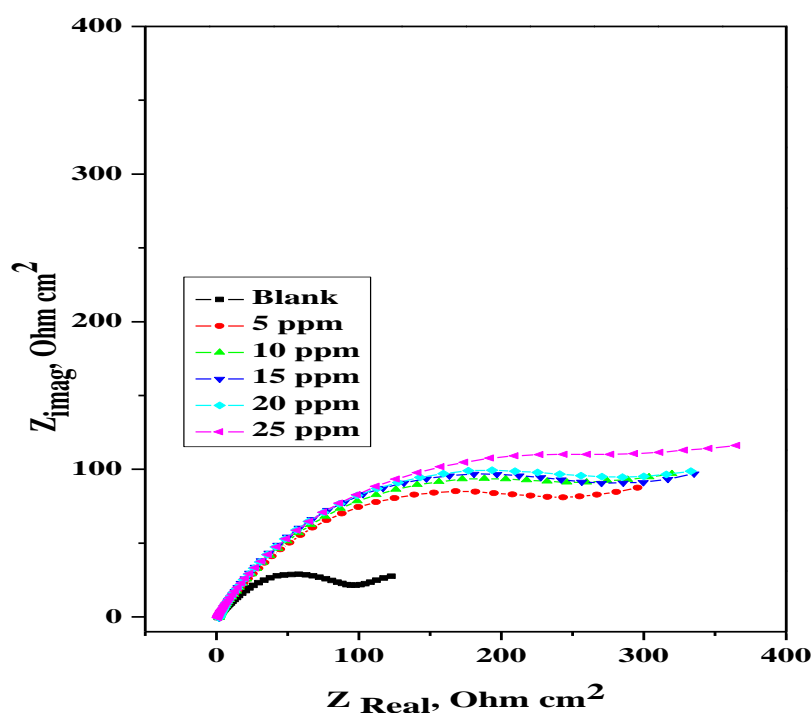
$C_{\text{inh}}$ , ppm	$-E_{\text{corr}}$ , mV vs SCE	$i_{\text{corr}}$ , mA cm <sup>-2</sup>	$-\beta_c$ , mV dec <sup>-1</sup>	$\beta_a$ , mV dec <sup>-1</sup>	CR, mmy <sup>-1</sup>	$\theta$	% IE
Blank	23	146.0	233	226	81.0	—	—
5	23	79.0	245	215	77.1	0.459	45.9
10	51	40.0	196	215	22.1	0.726	72.6
15	63	43.7	192	218	24.2	0.701	70.1
20	55	35.0	194	215	19.3	0.760	76.0
25	57	43.0	200	219	23.8	0.705	70.5

### 3.5 Electrochemical impedance (EIS) measurements

EIS plots (Nyquist and Bode plots) for Cu in 0.5 M HNO<sub>3</sub> without and with different concentrations of NOE at 30°C were presented in Figs. (7, 8). It is clear that the Nyquist plots (Fig. 7) did not display ideal semicircle, this may be because the frequency dispersion [33], which results from the surface roughness. From the plots, the diameter of the semicircle increases by addition of NOE indicating a barrier that formed on the Cu surface, which protects it from corrosion. The shape of the curves without and with NOE is very similar indicating that the presence of NOE does not change the corrosion mechanism [34]. The simple equivalent circuit model given in Fig. 9 was used to analyze the EIS spectra by fitting the experimental data. This circuit has the solution resistance ( $R_s$ ), ( $C_{dl}$ ) which is parallel ( $R_{ct}$ ) [35]. Bode plots (Fig. 8), the low-frequency limit represents ( $R_{ct} + R_s$ ), while the high-frequency limit represents ( $R_s$ ) Values of  $C_{dl}$  were calculated as follows:

$$C_{dl} = \frac{1}{2\pi f_{max} R_{ct}} \quad (10)$$

where  $f_{max}$  is the frequency at which the imaginary component of the impedance is maximum. The impedance parameters were listed in Table 6. As shown from the table, the value of  $R_{ct}$  increases with increasing NOE concentration, leading to an increase in %IE value. Decreasing value of  $C_{dl}$  in the presence of NOE may be because of the decrease in local dielectric constant and/or increasing the thickness of the double layer, which indicates that NOE inhibits the corrosion of Cu by adsorption at metal/acid [36,37].



**Figure 7.** Nyquist plots for Cu in 0.5 M HNO<sub>3</sub> without and with different concentrations of NOE

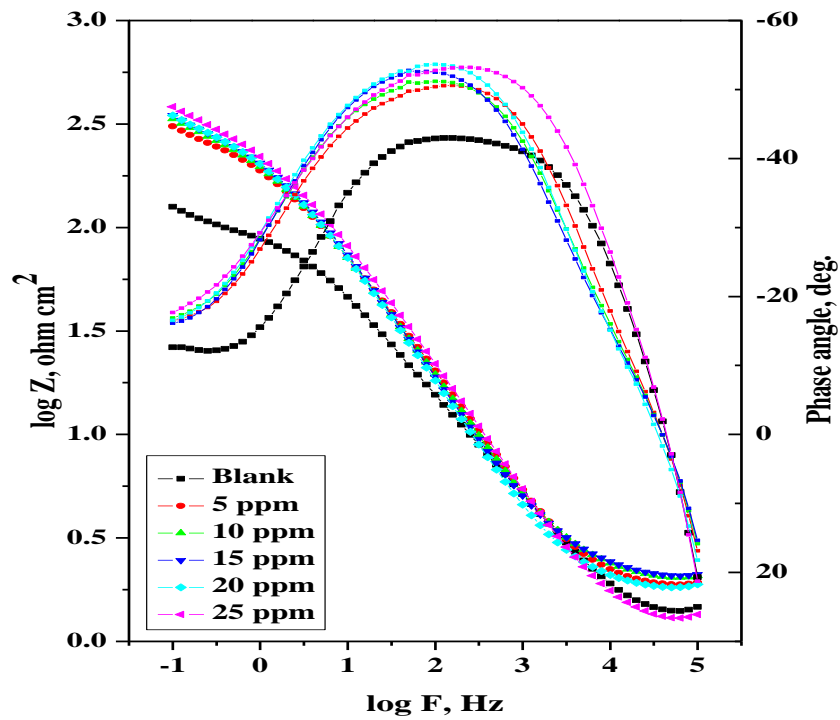


Figure 8. Bode plots for Cu in 0.5 M HNO<sub>3</sub> without and with different concentrations of NOE

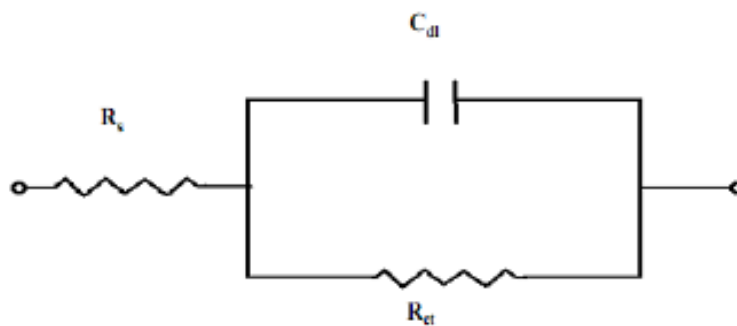


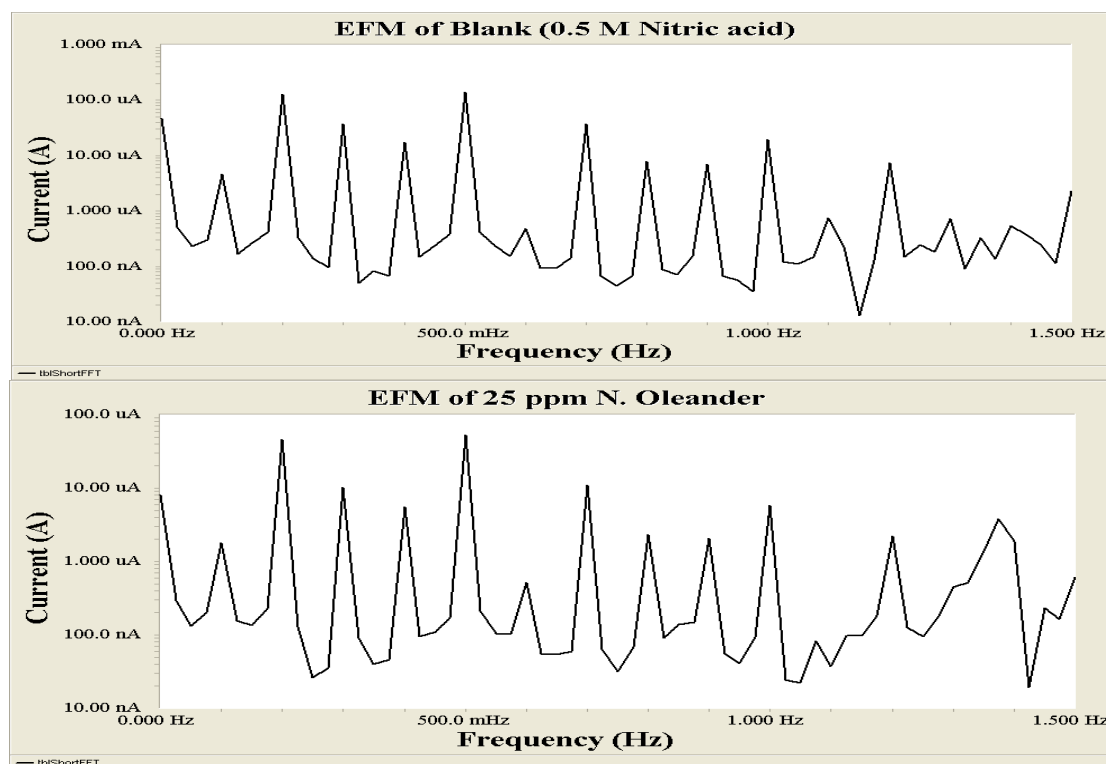
Figure 9. Equivalent circuit used in analyzing impedance spectra

Table 6. Corrosion parameters obtained from EIS measurements for Cu in 0.5 M HNO<sub>3</sub> without and with different concentrations of NOE

C <sub>inh</sub> , ppm	C <sub>dl</sub> , μF cm <sup>-2</sup>	R <sub>ct</sub> , Ω cm <sup>2</sup>	Θ	% IE
Blank	389	119.4	—	—
5	397	313	0.619	61.9
10	438	345.5	0.654	65.4
15	416	350.7	0.660	66.0
20	409	352.7	0.661	66.1
25	366	387.2	0.692	69.2

## 3.6 Electrochemical frequency modulation (EFM) measurements

Fig. 10 shows the EFM spectra for Cu in 0.5 M HNO<sub>3</sub> without and with different concentrations of NOE at 30°C. The parameters from EFM measurements ( $i_{\text{corr}}$ ,  $\beta_a$ ,  $\beta_c$ , CF-2, CF-3, CR,  $\theta$  and %IE) were listed in Table 7. It is observed from the data that, the value of  $i_{\text{corr}}$  decreases by increasing NOE concentration and %IE increases. If the causality factors are approximately equal to 2.0 and 3.0 for CF-2, CF-3, respectively, this indicates the presence of a causal relationship between the perturbation signal and the response signal, and the results are considered to be trusted [38]. Deviation of CF-2 and CF-3 values from ideality may be because the perturbation amplitude was overly small, or the frequency spectrum resolution is not sufficiently high, or the inhibitor is not working very well [39].



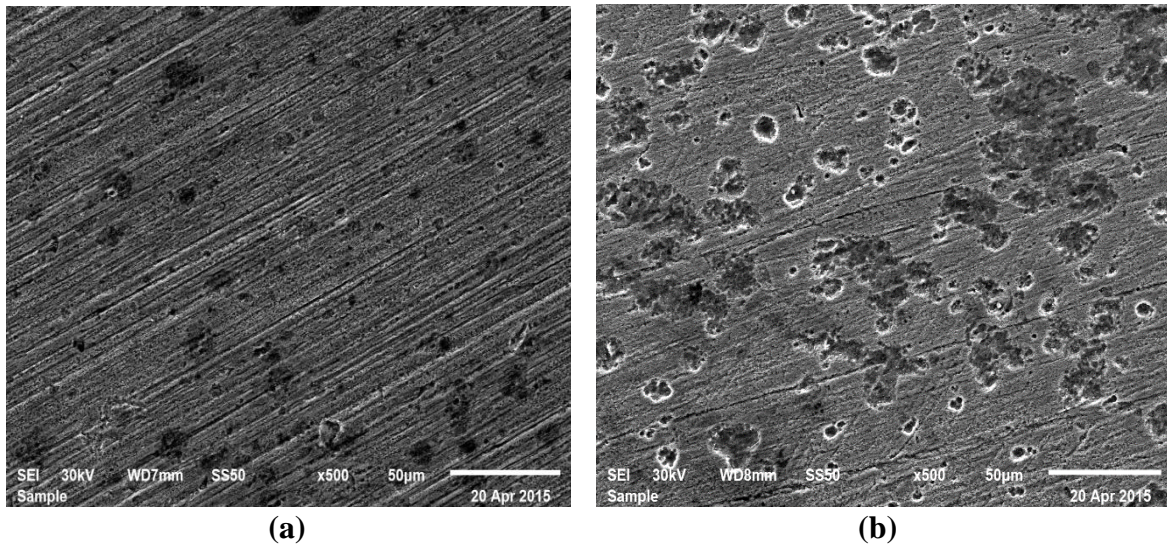
**Figure 10.** EFM spectra for Cu in 0.5 M HNO<sub>3</sub> without and with 25 ppm of NOE

**Table 7.** The corrosion parameters obtained from EFM

$C_{\text{inh}}$ , ppm	$i_{\text{corr}}$ , $\mu\text{Acm}^{-2}$	$\beta_c$ , $\text{mVdec}^{-1}$	$\beta_a$ , $\text{mVdec}^{-1}$	CF-2	CF-3	CR, $\mu\text{m}^{-1}$	$\theta$	% IE
Blank	163.4	253	47	2.01	4.86	90.35	—	—
5	65.09	150	50	1.90	2.84	35.99	0.602	60.2
10	61.42	164	52	1.88	3.87	33.96	0.624	62.4
15	58.08	159	53	1.86	2.92	32.11	0.645	64.5
20	57.37	136	48	1.88	2.83	31.72	0.649	64.9
25	55.14	139	49	1.89	3.80	30.49	0.663	66.3

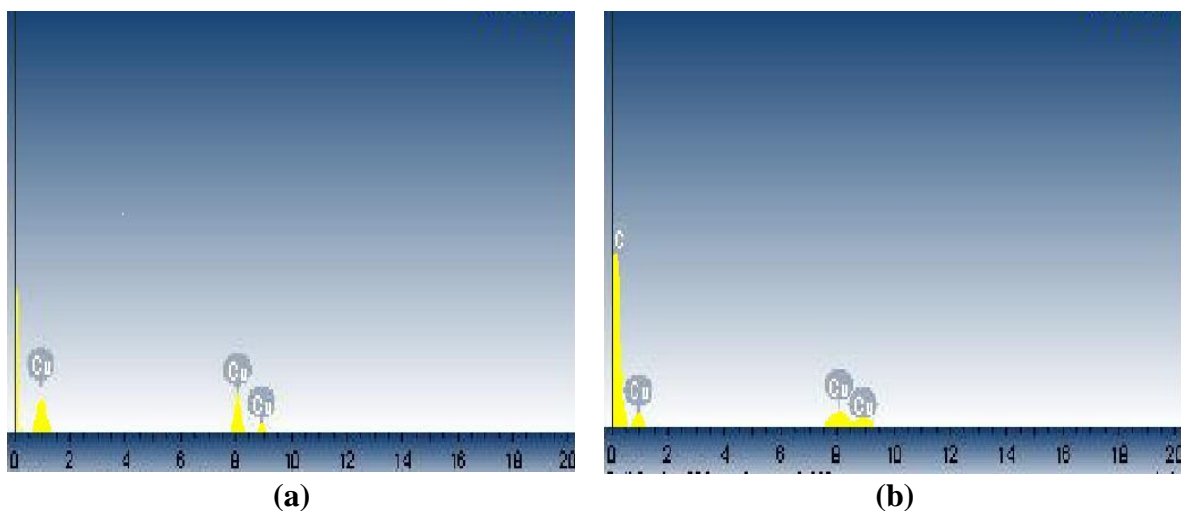
### 3.7 Scanning Electron Microscopy (SEM) Analysis

Scanning electron micrographs for corroded Cu surface without and with 25 ppm of NOE were illustrated in Fig. 11(a, b). The results appeared that the uninhibited Cu surface exhibits a very rough surface, this results from a corrosive attack by the nitric acid solution (Fig. 11(a)). The roughness of the inhibited Cu surface (Fig. 11(b)) decreases, this because a protective layer of NOE formed on the Cu surface. This layer decreases the surface roughness and protects the Cu from corrosion.



**Figure 11.** SEM (x500) for Cu exposed to 0.5M HNO<sub>3</sub> solution (a) without NOE (b) with 25 ppm NOE

### 3.8 Energy Dispersive X-ray (EDX) Analysis



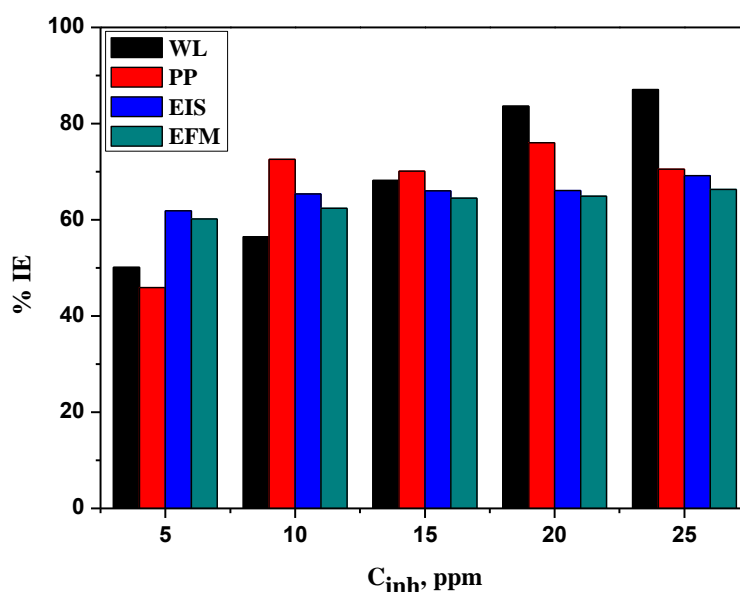
**Figure 12.** EDX analysis of Cu surface after exposure to 0.5 M HNO<sub>3</sub> solution (a) without NOE (b) with 25 ppm of NOE

Fig. 12(a) shows the EDX analysis for uninhibited Cu surface. The analysis indicates that only Cu was detected. The EDX analysis for Cu surface with 25 ppm of NOE is shown in Fig. 12(b). The figure illustrates the presence of peaks related to Cu and an additional line related to carbon. This indicated the presence of a protective film of NOE on the Cu surface. Table 8 represents the weight percentage (weight %) of Cu and carbon atoms in the protective films as obtained using EDX for Cu surface without and with the extract. It is clearly shown that Cu% on the surface decreases while carbon% increases with NOE. This indicates the replacement of the Cu atoms by NOE due to its adsorption on the Cu surface, which forms a protective film on it and hence reduces its corrosion.

**Table 8.** Weight percentage (weight %) of Cu and carbon atoms in the protective film as obtained using (EDX) for Cu surface without and with 25 ppm of NOE

Compound	Cu %	C %
Blank	100	—
Nerium oleander	21.01	78.99

Fig. 13 represents a comparison of %IE of different concentrations of NOE as obtained from the studied techniques. It is clear that the recorded values of %IE were in good agreement, indicating the validity of the studied techniques in examination of NOE as Cu corrosion inhibitor in 0.5 M HNO<sub>3</sub>



**Figure 13.** Comparison of %IE of different concentrations of NOE for Cu in 0.5 M HNO<sub>3</sub> as obtained from the studied techniques

### 3.9 Corrosion Inhibition Mechanism

Photochemical analysis of NOE indicated that the constituents that identified in the methanol extract of NOE plant (Table 1), have a lot of heteroatoms (O atoms), and donating groups such as: OH group, Cl group, CH<sub>3</sub> group, and  $\pi$ -electrons, that help in adsorption of NOE molecules on the Cu surface. The adsorption of extract molecules on Cu surface is physically due to  $\Delta G^{\circ}_{ads}$  is less than 20 kJ mol<sup>-1</sup>. So, the adsorption is due to the electrostatic attraction between the Cu surface and the extract molecules. The extract molecules may be protonated in acid medium. The Cu surface is positively charged in acid medium [40]. So, it is difficult to the protonated extract molecules to adsorb on the positively Cu surface. First NO<sub>3</sub><sup>-</sup> anions get adsorbed on Cu surface, the Cu surface become negatively charged, then the protonated extract molecules get adsorbed on the Cu surface and cover large surface area. Table 9 shows a comparison between values of %IE of some plant extracts for Cu corrosion in HNO<sub>3</sub>. As shown from the table, NOE is an effective inhibitor for Cu corrosion in HNO<sub>3</sub>.

**Table 9.** Comparison between %IE of some plant extracts for Cu corrosion in HNO<sub>3</sub>

Plant extract	C <sub>inh</sub>	[HNO <sub>3</sub> ]	%IE	Reference
Hyoscyamus Muticus Extract (HME)	50 ppm	1 M	43.0	41
Artemisia Essential Oil	50 ppm	2 M	48.2	42
Carapichea Ipecacuanha Extract (CIE)	25 ppm	1 M	55.5	43
Senesio Extract	11 x 10 <sup>-6</sup> M	1 M	77.5	44
Nerium oleander extract	25 ppm	0.5 M	87.1	Our results

## 4. CONCLUSIONS

NOE was tested (using WL method, electrochemical techniques, and surface studies) as inhibitor for Cu corrosion in 0.5 M HNO<sub>3</sub>. Results showed that:

NOE is an effective corrosion inhibitor for Cu in 0.5 M HNO<sub>3</sub>. Corrosion rate increases with temperature, and decreases with increasing NOE concentration and hence, %IE increases. Adsorption of NOE on Cu surface followed Frumkin adsorption isotherm and the apparent activation energy increases with increasing the extract concentration suggesting physisorption. Anodic and cathodic curves with NOE were shifted toward both positive and negative potentials, indicating a mixed type inhibitor mechanism. Values of %IE from the studied techniques showed similar range, indicating the validity of the studied techniques in examining the inhibiting action of NOE towards the dissolution of Cu in 0.5 M HNO<sub>3</sub>.

## References

1. A. Fiala, A. Chibani, A. Darchan, A. Boulkamh, K. Djebbar, *Appl. Surf. Sci.*, 253 (2007) 9347
2. K.F. Khaled, *Corros. sci.*, 52 (2010) 3225-3234
3. M. Mihit, L. Bazzi, R. Salghi, B.Hammouti, S. El Issami, E. Ait Addi, *Int. Sci. J. Altern. Ener. Ecol. (ISJAE)*, 62 (2008) 173-181
4. M.M. El-Naggar, *Corros. Sci.*, 42 (2000) 773-784



5. A.S. Fouda, A. Abd El-Aal, A.B. Kandil, *Desalination*, 201 (2006) 216-223
6. K. Barouni, M. Mihit, L. Bazzi, R. Salghi, B. Hammouti, A. Albourine, S. El Issami, *Mater. lett.*, 62 (2008) 3325-3327
7. K.F. Khaled. *Electrochim. Acta*, 54 (2009) 4345
8. M. Mihit, R. Salghi, S. El Issami, *Pigm. Resin. Technol.*, 35(3) (2006) 151-157
9. O.R.M. Khalifa, A.K. Kassab, H.A. Mohamed, S.Y. Ahmed, *Journal of American science*, 6(8) (2010) 487-498
10. K. Barouni, M. Mihit, L. Bazzi, R. Salghi, S.S. Al-Deyab, B. Hammouti, A. Albourine, *The open corrosion journal*, 3 (2010) 58-63
11. A. Zarrouk, B. Hammouti, H. Zarrok, M. Bouachrine, K.F. Khaled, S.S. Al-Detab, *Int. J. Electrochem.*, 7 (2012) 89-105
12. B.V. Appa Rao, Md. Yakub Iqbal, B. Sreedhar, *Electrochim. Acta*, 55(3) (2010) 620-631
13. J.S. Chauhan, *Asian Journal of Chemistry*, 21 (2009) 1975-1978
14. T.V. Sangeetha, M. Fredimoses, *E-Journal of Chemistry*, 8(S1) (2011) S1-S6
15. Fernando Silvio de Souza, Cristiano Giacomelli, Reinaldo Simões Gonçalves, Almir Spinelli. *Mater. Sci. Eng.*, 32 (2012) 2436-2444
16. B.A. Abd-El-Nabey, A.M. Abdel-Gaber, M. El Said Ali, E. Khamis, S. El-Housseiny, *J. Electrochem. Sci.*, 8 (2013) 5851-5865
17. L.Valek, S. Martinez, *Mater. Lett.*, 61(1) (2007) 148-151
18. A.S. Fouda, M.A. Elmersi, B.S. Abou-Elmagd, *Pol. J. Chem. Tech.*, 19(1) (2017) 95-103
19. Savita, Namrata Chaubey, Punita Mourya, V.K. Singh, M. M. Singh, *International Journal of Innovative Research in Science, Engineering and Technology (IJIRSET)*, 4(6)(2015)4545-4553
20. Fadel Wedian, Mahmoud A. Al-Qudah and Ghassab M. Al-Mazaideh, *Int. J. Electrochem. Sci.*, 12 (2017) 4664 – 4676
21. A.S. Fouda, K. Shalabi, A.A. Idress, *Green Chem. Lett. Rev.*, 8(3-4) (2015) 17-29
22. E.E Oguzie, *Corros. Sci.*, 49(3) (2007) 1527–1539
23. H. Ashassi-Sorkhabi, B. Shaabani, D. Seifzadeh, *Appl. Surf. Sci.*, 239 (2005) 154–164
24. H. Zarrok, A. Zarrouk, B. Hammouti, R. Salghi, C. Jama, F. Bentiss, *Corros. Sci.*, 64 (2012) 243–252
25. M.M. Fares, A.K. Maayta, M.M. Al-Qudah, *Corros. Sci.*, 60 (2012) 112
26. M. Behpour, S.M. Ghoreishi, M. Khayat Kashani, N. Soltani, *Mater. Chem. Phys.*, 131 (2012) 621-633
27. S. Garai, P. Jaisankar, J.K. Singh and A. Elango, *Corros. Sci.*, 60 (2012) 193-204
28. M.K. Gomma, M.H. Wahdan, *Mater. Chem. Phys.*, 39 (1995) 209–213
29. E.M. Blomgren, J.O. Bockris, C. Jesch, *J. Phys. Chem.*, 65 (1961) 20–25
30. A. Popova, E. Sokolova, S. Raicheva and M. Christov, *Corros. Sci.*, 45 (2003) 33-58
31. I. Ahamad, R. Prasad, M.A. Quraishi, *Corros. Sci.*, 52 (2010) 1472-1481.
32. A.S. Fouda, M.A. El-Morsy, A. A. El-Barbary and Lamia E. Lamloum, *Int. J. Corros. Scale Inhib.*, 5(2) (2016) 112-131
33. T. Paskossy, *J. Electroanal. Chem.*, 364 (1994) 111-125
34. A.J. Trowsdate, B. Noble, S.J. Haris, I.S.R. Gibbins, G.E. Thomson, G.C. Wood, *Corros. Sci.*, 38(2) (1996) 177-191
35. I. Sekine, M. Sabongi, H. Hagiuda, T. Oshibe, M. Yuasa, T. Imahc, Y. Shibata, T. Wake, *J. Electrochem. Soc.*, 139 (1992) 3167
36. M. Lagrenee, B. Mernari, M. Bouanis, M. Traisnel, F. Bentiss, *Corros. Sci.*, 44(3) (2002) 573-588
37. M. N. El-Haddad, A. S. Fouda, *J. Mol. Liq.*, 209 (2015) 480-486
38. R.W. Bosch, J. Hubrecht, W.F. Bogaerts, B.C. Syrett, *Corrosion*, 57(1) (2001) 60-70
39. S.S Abdel-Rehim, K.F Khaled, N.S Abd-Elshafei, *Electrochim. Acta*, 51 (2006) 3269–3277
40. Da-quan Zhang, Li-xin Gao, Gao-ding Zhou, *Corros. Sci.*, 46 (2004) 3031-3040
41. A.S. Fouda, Y.M. Abdallah, G.Y. Elawady, R.M. Ahmed, *J. Mater. Environ. Sci.*, 5 (6) (2015) 1519-

1531

42. Sara Houbairi, Mohammed Essahli, Abdeslam Lamiri, *International Journal of Engineering Research & Technology (IJERT)*, 3 (1) (2014) 1527-1538
43. R.M. Younis, Hala.M. Hassan, R.A. Mansour, A.M. El-desoky, *International Journal of Scientific & Engineering Research (IJSER)*, 6(9) (2015)761-770
44. A.S. Fouda, H.M. Kila, A. Attia, A.M. Salem, *Corrosion & Dye*, 83 (2015) 32747-32754

© 2019 The Authors. Published by ESG ([www.electrochemsci.org](http://www.electrochemsci.org)). This article is an open access article distributed under the terms and conditions of the Creative Commons Attribution license (<http://creativecommons.org/licenses/by/4.0/>).